

Solar probe mission: Close encounter with the Sun

E. C. Sittler Jr.¹, D. J. McComas² and R. L. McNutt Jr.³ and the STDT Team

¹ NASA Goddard Space Flight Center, Greenbelt, MD, USA

² Southwest Research Institute, San Antonio, TX, USA

³ Applied Physics Laboratory, Laurel, MD, USA

Abstract. The Solar Probe Science and Technology Definition Team (STDT) recently completed a detailed study of the Solar Probe Mission based on an earliest launch date of October 2014. Solar Probe, when implemented, will be the first close encounter by a spacecraft with a star (i.e., $3 R_S$ above the Sun's photosphere). The report and its executive summary were published by NASA (NASA/TM-2005-212786) in September 2005 and can be found at the website <http://solarprobe.gsfc.nasa.gov/>. A description of the science will appear in *Reviews of Geophysics* article led by D. J. McComas. For this talk, we presented the consensus view of the STDT including a brief description of the scientific goals, a description of the overall mission, including trajectory scenarios, spacecraft description and proposed scientific payload. We will discuss all these topics and the importance of flying the Solar Probe mission both with regard to understanding fundamental issues of solar wind acceleration and coronal heating near the Sun and Solar Probe's unique role in understanding the acceleration of Solar Energetic Particles (SEPs), which is critical to future Human Exploration.

Index Terms. Human exploration, space weather, solar corona, solar energetic particles, solar wind.

1. Introduction

The Solar Probe Mission, when implemented, will truly be a mission of discovery where it will venture into the innermost regions of the heliosphere of the Sun, where no spacecraft has ever gone before. The mission has the scientific potential for changing the paradigm of our understanding of coronal heating and solar wind acceleration. This mission is a high technology mission, where it must withstand at perihelion, $r \sim 4 R_S$, photon intensities ~ 3000 Suns when compared to that at Earth, such that its Thermal Protection System (TPS) or heat shield will acquire temperatures $\sim 1800^\circ\text{K}$, while the spacecraft bus and scientific instruments will operate near room temperature $T < 50^\circ\text{C}$. The spacecraft, which will be in a polar orbit, will be moving at speeds exceeding 300 km/s at perihelion and must withstand dust impacts from the surrounding dust environment normally attributed to the zodiacal light and F corona routinely observed by solar coronagraph imagers. The STDT (Solar Probe Science and Technology Definition Team) study has determined that the spacecraft will perform well under these extreme environmental conditions with significant margins of safety. Solar Probe is required for a complete understanding of the Sun's atmosphere, corona and solar wind at its most fundamental levels of physical understanding. Furthermore, Solar Probe will provide ground truth observations for remote sensing observations of the Sun, the latter of which is planned to occur during the perihelion passes of the Sun by Solar Probe. For example, Solar Orbiter ESA mission is presently planned to be in position to image the corona at 2018 when Solar Probe is planned to make its first perihelion

pass with the Sun. Coordination with this and/or any other solar observing missions will significantly enhance the science return of all missions. Such achievements may then allow routine space weather predictions of the Sun's activity, CME and SEP prediction, based on remote sensing observations of the Sun. This capability will be an essential ingredient for a sustained human presence in space as envisioned by NASA in the coming decades.

In this brief report, we will present highlights of the STDT study results with regard to scientific goals, a description of the overall mission including launch, trajectory, spacecraft description and proposed scientific straw man payload. In the initial "Simpson Report" for NASA back in 1958, Solar Probe was recognized as being necessary to understand coronal heating and solar wind acceleration. Most recently, the mission has been given the highest priority by the National Research Council (NRC) Decadal Report as the next large flagship mission in heliospheric physics to be implemented as soon as possible. It has also been recommended by numerous NASA committees of late.

The paper will begin by first presenting the mission concept before the science rationales are given. This will put the science rational in perspective with regard to mission capabilities, which will then justify the proposed mission concept a priori. The science rationale will be followed by a section focused on human exploration and why Solar Probe must be done as soon as possible.

2. Mission implementation

2.1 Solar probe spacecraft

The straw man design of the Solar Probe spacecraft is shown in Fig. 1. The spacecraft is composed of a cone shaped carbon-carbon heat shield which is coated, for example, by an Al_2O_3 coating, to provide an $\alpha/\epsilon \sim 0.6$, (i.e., absorption coefficient in visible the wavelength band divided by emissivity in infrared wavelength band) so that the heat shield will operate at temperatures $T < 1800$ °K. At the base of the conical heat shield is the secondary heat shield (SHS) which achieves a temperature $\sim 500^\circ\text{C}$ at its lower surface, which is then covered by high temperature MLI. This reduces the heat input to the bus from the SHS to less than 26 watts.

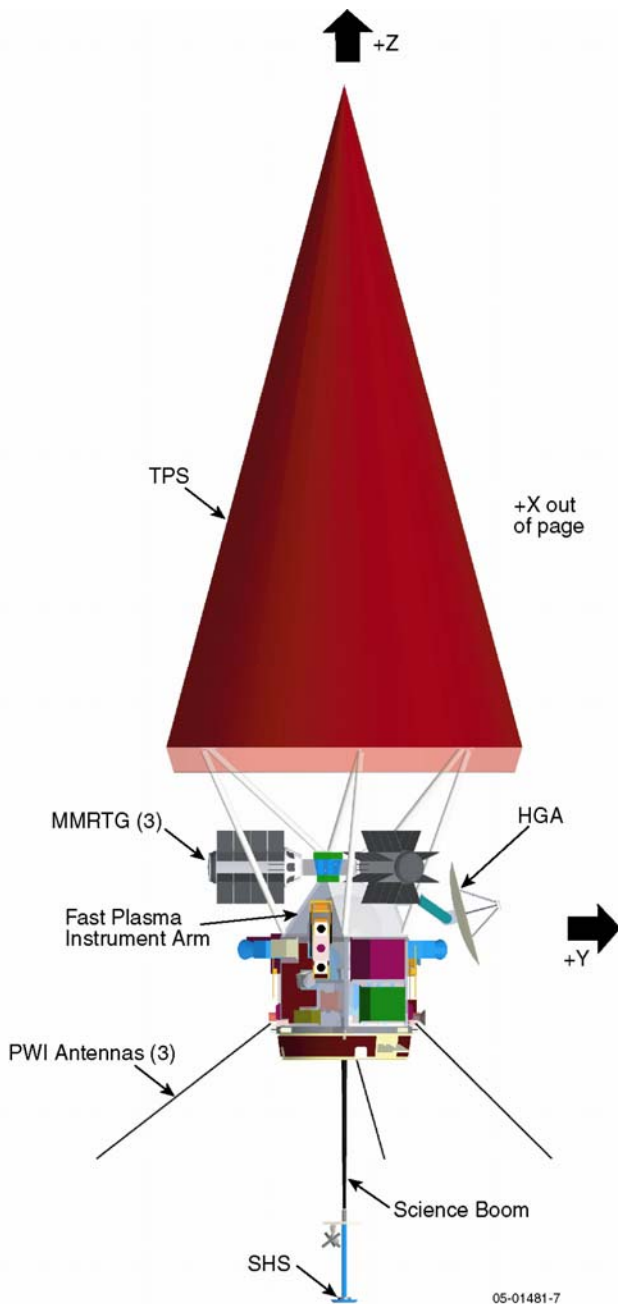


Fig. 1. Solar Probe spacecraft showing TPS, cluster of 3 MMRTGs, cylindrical bus, science boom and PWI antennas (3) deployed.

Between the secondary heat shield and the top deck of the spacecraft bus is located three MMRTGs spaced 120° apart around the symmetric Z-axis of the spacecraft. The three MMRTGs provide ~ 316 watts of electricity to the spacecraft and scientific instruments. They radiate about 30 watts of heat to the spacecraft bus. The spacecraft bus has a cylindrical shape and is where the scientific instruments are located. The mass, power and telemetry rate of the different instruments are listed in Table 1. (Table does not include 4.5 kg for PWI electric field antennas.) The total launch mass including fuel is ~ 856 kg. Aft of the spacecraft bus is a boom pointing anti-sunward with magnetometer and plasma wave search coil mounted near its end. At the end of the boom is located the solar horizon sensor (SHS) which is used as back up, if it were to venture outside the TPS umbra, to warn the spacecraft computer that its attitude is tilting outside its allowed nadir alignment with respect to the Sun and make corrective action. This feature is important to protect against unexpected anomalies. For example, “coronal light” could confuse the star trackers near perihelion.

2.2 Launch and trajectory scenario

As shown in Fig. 2, the spacecraft could be launched as early as October 11, 2014 from Cape Canaveral Florida. An Atlas 551 or Delta IV Heavy launch vehicle with STAR 48B third stage will be used to inject the spacecraft on a trajectory to Jupiter. The launch window is 20 days long with opportunities occurring every 13 months. The orbit C3 is ~ 125 km^2/sec^2 . Then on March 15, 2016, the spacecraft will receive a gravity assist from Jupiter (i.e., periapsis $\sim 12 R_J$ to avoid its radiation belts) where it will be directed to the Sun with polar orbit and perihelion distance of $4 R_S$ on November 26, 2018. Orbital period will be ~ 4.5 years. This first pass will occur near Solar Minimum. Fig. 3 shows the geometry of the first pass and Earth 15° from quadrature to allow simultaneous observations of the Sun’s corona from Earth. For this launch date there will be a second pass on July 15, 2023 when the Sun will be near Solar Maximum.

2.3 Data acquisition

The first pass geometry will be favorable for a real-time telemetry link to the Earth at 25 kbits/s. This will be done using the high gain antenna with Ka-band being used for the downlink. Ka-band is used since it is virtually immune to scintillation effects. The spacecraft will also have an X-band capability for both uplink and downlink. X-band will use both the low and medium gain antennas, in addition to using the high gain antenna when needed. The spacecraft computer and solid state recorder (SSR) and other critical sub-systems are doubled up as a risk reduction strategy and to ensure acquisition of all critical data on the ground that is recorded within $60 R_S$ of the Sun. All data will be stored in double buffered 128 Gbits of SSR memory (i.e., 256 Gbits total). The first pass is more favorable for returning ~ 121 Gbits of stored data to the ground, while the second pass is less favorable with ~ 57.4 Gbits telemetered to the ground for a total downlink ~ 101 days with ~ 8 hours of tracking per day to the Deep Space Network (DSN).

2.4 Scientific instruments

As listed in Table 1 we have six *in situ* instruments and two remote sensing instruments. The *in situ* plasma instrument package is composed of one Fast Ion Analyzer (FIA; $50 \text{ V} < E/Q < 20 \text{ kV}$), two Fast Electron Analyzers (FEA; $1 \text{ eV} < E < 5 \text{ keV}$) and one Ion composition Analyzer (ICA; $100 \text{ V} <$

$E/Q < 60 \text{ kV}$). The energetic particle instrument (EPI) is composed of an EPI low-energy instrument (EPI-Lo; $20 \text{ keV/nucleon} < E < 1 \text{ MeV/nucleon}$) and an EPI high energy instrument (EPI-Hi; $1 \text{ MeV/nucleon} < E < 100 \text{ MeV/nucleon}$). There is a DC Magnetometer (MAG; $0 < f < 20 \text{ Hz}$) and Plasma Wave Instrument (PWI).

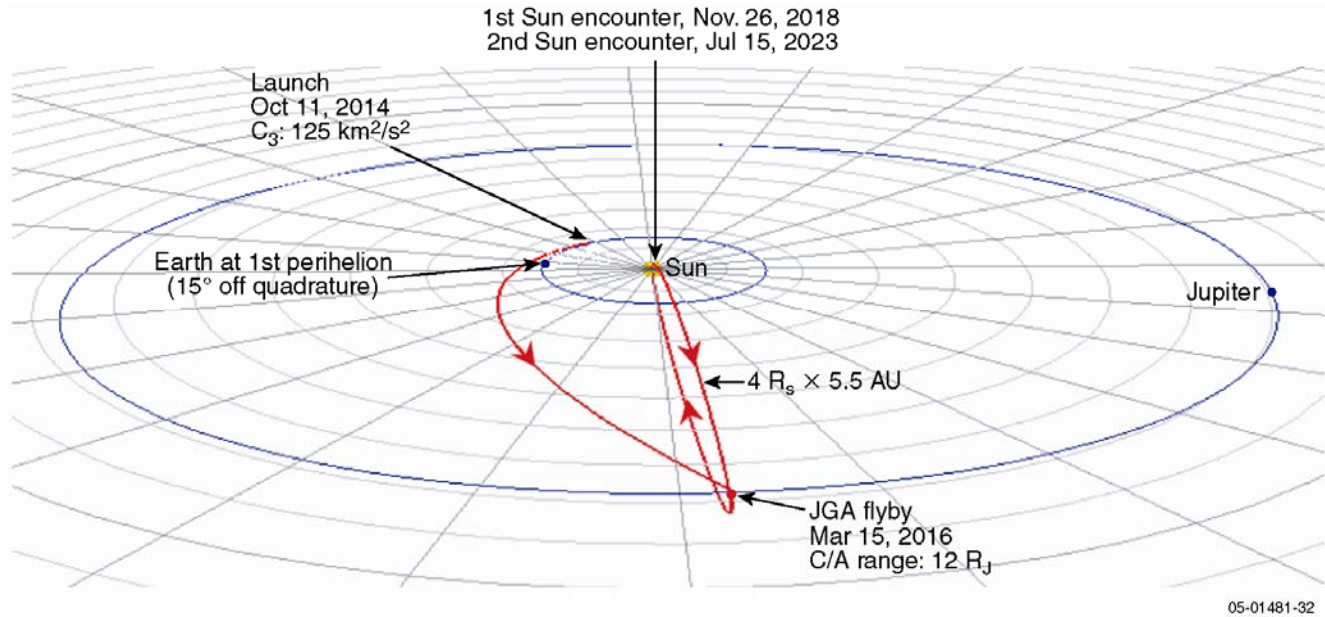


Fig.2a. Solar Probe launch, interplanetary trajectory, Jupiter Gravity Assist (JGA) and encounter with Sun. (b) Close-up views for solar encounter trajectory with science operations between ± 5 days of perihelion. Shows polar orbit with approach from South Pole.

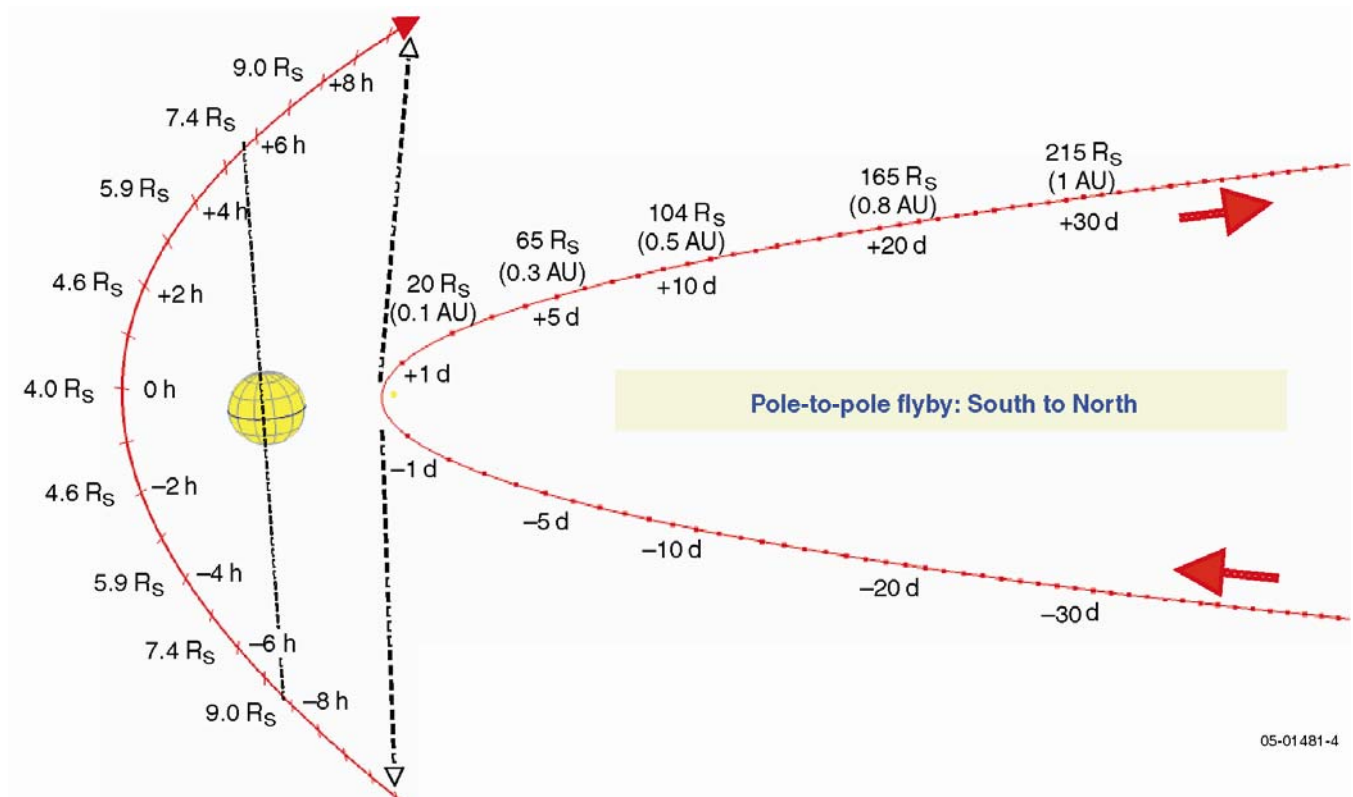


Fig.2b. Geometry of first solar encounter with Earth positioned 15° from quadrature to allow simultaneous observations from Earth.

The PWI is composed of three electric field antennas (shown deployed in Fig. 1; $1 \text{ Hz} < f < 10 \text{ MHz}$) and search coil for electromagnetic wave detection ($1 \text{ Hz} < f < 80 \text{ kHz}$). Located behind the hydrazine tank of the spacecraft (used as moderator for fast neutrons) is located a Neutron/Gamma-Ray Spectrometer (NGS) to measure γ -rays ($1 \text{ MeV} < E < 100 \text{ MeV}$) and neutrons ($1 \text{ MeV} < E < 100 \text{ MeV}$). This instrument will be used to remotely detect nanoflares ($E \sim 10^{24}$ ergs) to large flares (Class X); the latter can produce Coronal Mass Ejections (CME). Finally, the *in situ* package includes a Coronal Dust Detector (CDD; 10^{-19} grams $< M < 10^{-12}$ grams) to detect the dust environment near the Sun and inner heliosphere. The PWI can also detect dust particle impacts on the spacecraft body, but with less precision. Dust impacts are expected to peak near the Sun's equator with a majority coming from the direction of planetary orbital motion (prograde motion).

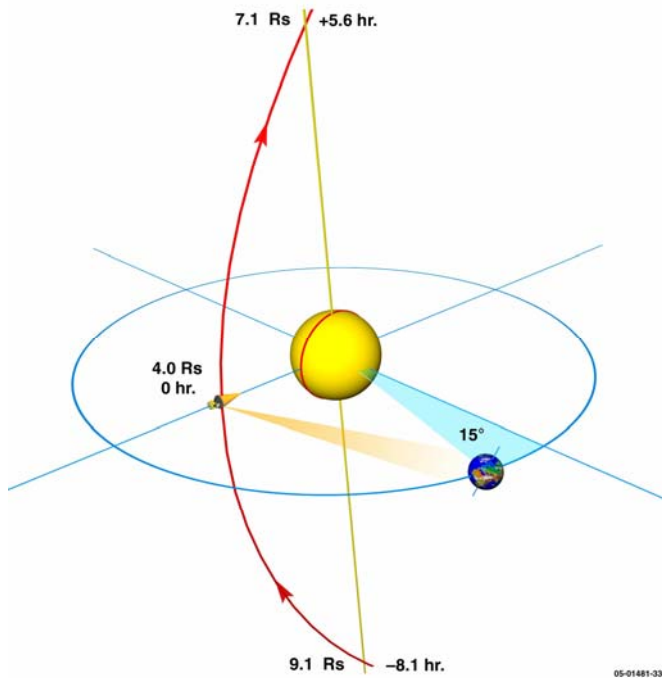


Fig. 3. Geometry of first solar encounter with Earth positioned 15° from quadrature to allow simultaneous observations from Earth.

The remote sensing package is composed of a white light coronagraph called the Hemispherical Imager (HI) and EUV-Magnetogram Imager called Polar Source Region Imager (PSRI). The PSRI makes measurements of the Sun's polar region between $20 R_S < r < 65 R_S$. Using a deployable mirror that extends outside the umbra, it takes images and then retracts, allowing the mirror to cool. This is repeated up to every 10 minutes. This instrument will allow one to measure the loop structure from the photosphere to the lower corona and photospheric magnetic fields over the poles. The HI will take 3D images of the coronal structure by taking advantage of the rapid change in image perspective as the spacecraft makes its fast scan from pole to pole of the Sun (i.e., 16 hours). Combined with ground based and near Earth

spacecraft images of the Sun's corona, these measurements will help separate time-space ambiguities in the *in situ* measurements.

The total mass and power of the scientific instruments is ~ 51 kg and ~ 57 watts, respectively. This includes doubly redundant science Common Data Processing Unit (CDPU) which includes power distribution unit and processor board with memory. Finally, 30% margin is added to these numbers for a final mass ~ 67 kg and final power ~ 74 watts allocation for the science package.

Table 1. Science Instruments

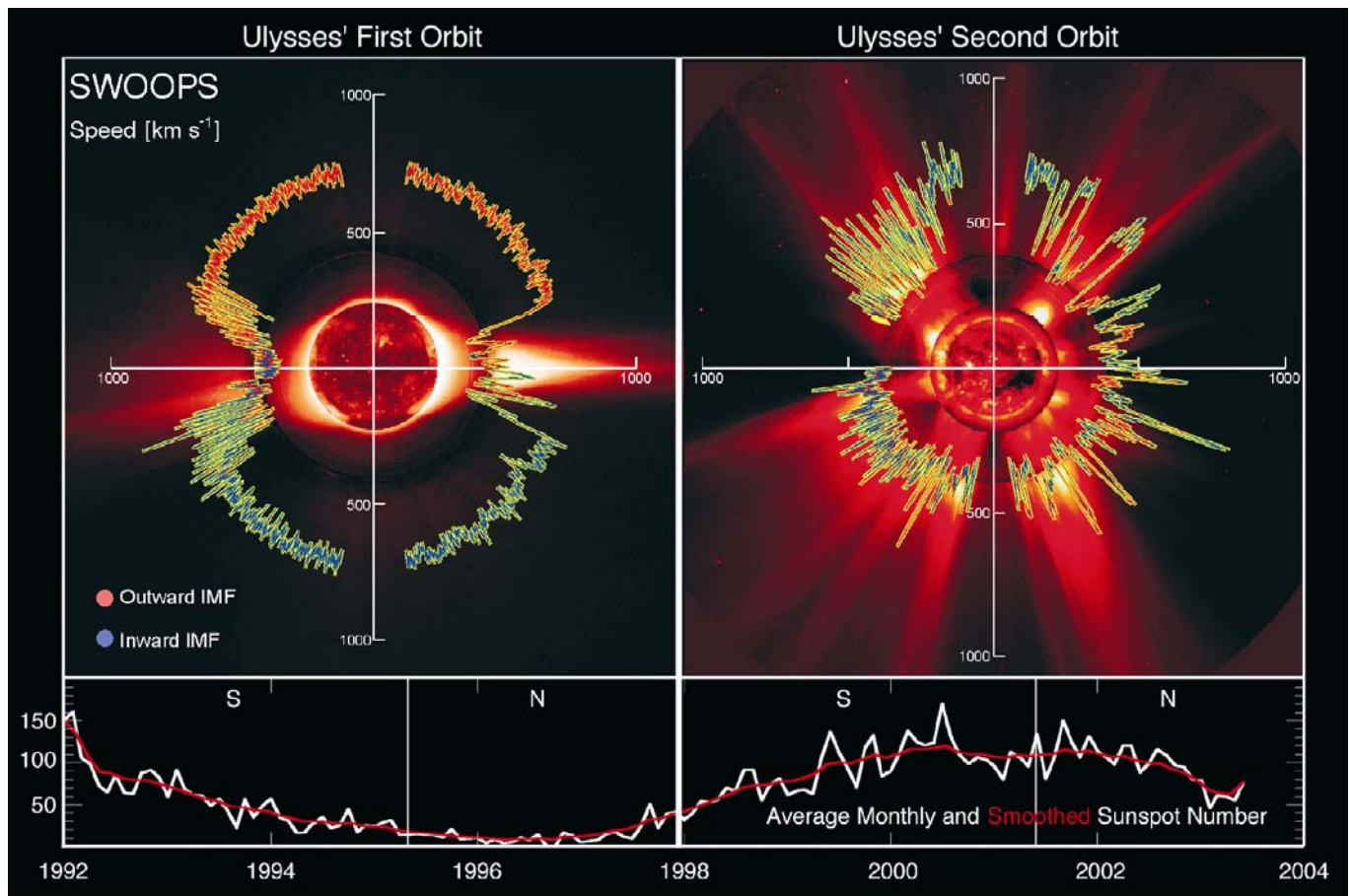
Instrument	Mass (kg)	Power (W)	Peak Data Rate (kbps)
Fast Ion Analyzer (FIA)	2.8	3.7	10
Fast Electron Analyzer (FEA)	5.0	7.2	20
Ion Composition Analyzer (ICA)	7.0	6.0	10
Magnetometer (MAG)	2.5	2.5	1.1
Plasma Wave Instrument (PWI)	5.0	5.0	3.5
Energetic Particle Instrument Low Energy (EPI-Lo)	1.4	2.3	5
Energetic Particle Instrument High Energy (EPI-Hi)	2.7	1.7	3
Neutron/Gamma Ray Spectrometer (NGS)	2.0	3.0	0.5
Coronal Dust Detector (CD)	1.5	3.8	0.1
Hemispheric Imager (HI)	1.5	4.0	70
Polar Source Region Imager (PSRI)	3.5	4.0	70
Common DPU/LVPS	10.8	14.0	N/A
Total	45.7	57.2	123.2

3. Science requirements

The Solar Probe Science Objectives can be summarized into four major goals: 1) Determine the structure and dynamics of the magnetic fields at the sources of the solar wind; 2) Trace the flow of the energy that heats the solar corona and accelerates the solar wind; 3) Determine what mechanisms accelerate and transport energetic particles; and 4) Explore dusty plasma phenomena and their influence on the solar wind and energetic particle formation. We will briefly describe each objective separately.

3.1 Determine structure and dynamics of magnetic field and solar wind sources

As shown in Fig. 4 we have a composite figure of coronagraph, EUV and Ulysses solar wind data showing the structure of the corona and solar wind (McComas *et al.*, 2003). This figure clearly shows the difference in structure for solar minimum and solar maximum. During solar minimum, the corona displays a very simple structure with a single equatorial streamer of slow wind and polar region of high-speed solar wind with unipolar regions of positive magnetic polarity within north polar coronal holes and negative polarity in south polar coronal holes. During solar maximum, one sees streamers at all latitudes and complex mixtures of high-speed and slow-speed solar wind. The magnetic polarity also shows a complex structure with latitude. The high-speed winds with $V \sim 800 \text{ km/s}$, cannot be explained as a thermally driven wind



05-01481-68

Fig.4. Composite plot of Ulysses solar wind speed, density and magnetic field polarity super-imposed on solar images by SOHO EIT and LASCO C2 and Mauna Loa K-coronameter (McComas et al., 2003).

as originally proposed by Parker (1958). The high-speed wind during solar minimum is observed to be very steady and uniform, while for slow wind, $V \sim 400$ km/s, is more structured and time dependent. Observations of ion charge state by the Ulysses SWICS experiment during solar minimum (Geiss et al., 1995) show the coronal electron temperature to be cooler over the poles and hotter near the equator, which is opposite of what one would expect for a thermally driven wind. The First Ionization Potential (FIP) effect using ion composition measurements by Ulysses and ACE, shows an enhancement for slow wind relative to high-speed wind or polar coronal holes, which can be explained by larger coronal loops reconnecting with open field structures near the equator, and smaller coronal loops reconnecting with open field structures over the poles (Zurbuchen et al., 2002; Schwadron et al., 1999).

One also wants to study the expansion factor of the field which tends to anti-correlate with solar wind speed (Wang et al., 1997). Solar Probe will be able to confirm this empirical relationship by measuring the magnetic field and solar wind flow along the spacecraft trajectory as it approaches the Sun and passes over the Sun's poles. Furthermore, the expansion factors are based on magnetogram observations and potential source surface (PSS) calculations. Solar Probe will be able to

confirm this modeling technique. Other approaches use a force free approach where currents cannot be ignored. Solar Probe will be able to validate, or invalidate, the above techniques, which are used to model coronal magnetic fields. Similarly, Solar Probe can measure the density, flow velocity and temperature of the ion-electron gas along its trajectory to understand how the corona is heated and solar wind accelerated.

3.2 Trace flow of energy that heats the corona and accelerates the solar wind

Numerous models have been proposed for heating the corona and accelerating the solar wind. The flow of energy and momentum flux from the base of the corona is critical to how the above happens. Some models invoke waves propagating from photospheric heights where granular and super-granular motions are observed (Hollweg, 1974, 1978). Unfortunately fast and slow mode waves are dissipated before they can reach coronal heights, and only Alfvén waves can propagate to the corona and solar wind. Solar wind acceleration via a wave pressure term by Alfvén waves was originally proposed by Belcher (1971). But, Alfvén wave observations by Helios showed there was insufficient energy in the waves to account for the observed high-speed winds (Roberts, 1989). But, it is

well established that Alfvén waves dominate MHD waves

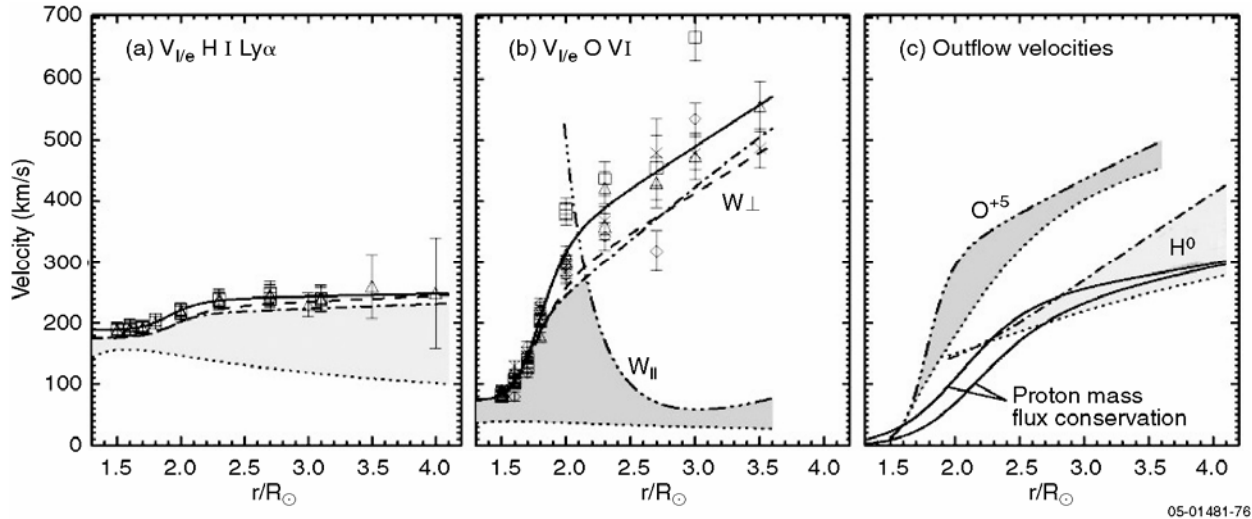


Fig. 5. SOHO/UVCS emission line width observations by Kohl *et al.* (1998). Shaded regions indicate uncertainties due to thermal broadening. Error bars are shown.

observed within high-speed streams (Hollweg and Isenberg, 2002). Solar Probe will pass through the polar region inside the Alfvén critical point where Alfvén wave amplitudes are expected to maximize with $\delta V \sim 200\text{--}300$ km/s (Cranmer and van Ballegoijen, 2005). Furthermore, outward propagating Alfvén waves can be reflected at the Alfvén critical point and one can expect both outward and inward propagating Alfvén waves within the polar region sampled by Solar Probe (i.e., sub-Alfvénic flow). Matthaeus *et al.* (1999) have shown, when oppositely propagating Alfvén waves exist, turbulence can occur with the turbulence cascading to higher wave numbers, which can then produce local small scale reconnection events. Under such conditions one may expect to see nanoflares both moving away from the Sun and toward the Sun. Only Solar Probe can make such measurements.

Another competing model is that by Parker (1988, 1991), where he has invoked the occurrence of reconnection events within the photospheric network, producing nanoflares to microflares. The small flares will then propagate to coronal heights in the form of ion jets (Parker, 1991) moving along open magnetic fields. These ion jets will then deposit their energy within the corona and heat it. As they dump their energy within the corona, they will generate wave turbulence and Alfvén waves which can then propagate into the solar wind and provide further acceleration of the solar wind to high-speed winds $V \sim 800$ km/s at heights $\sim 10 R_S$. Over the poles sampled by Solar Probe, $r \sim 8 R_S$, the Alfvén speed can exceed $V_A \sim 1000$ km/s. This means that field aligned ion jets can exceed the local flow speed of the plasma by as much as 1000 km/s. Only Solar Probe can make these measurements and distinguish between the various models.

These effects can be inferred by SOHO UVCS observations using a Doppler dimming effect for both protons and OVI (Kohl *et al.*, 1998) as shown in Fig. 6. OVI is a minor ion species, which is clearly seen to exceed the flow speed for protons by several hundred km/s. The OVI

also appears to be $\sim 5\text{--}10$ times hotter than the protons. This enhanced heating could be a complicated function of mechanical motions (i.e., Alfvén waves) and thermal motions of the gas. Only Solar Probe can uniquely separate these two effects. The heating mechanism proposed for the oxygen data is outward propagating ion cyclotron waves (Cranmer *et al.*, 1999). Solar Probe, with its plasma MAG and PWI instruments, has the capability to measure and identify the wave modes over the poles of the Sun, since the proton Doppler dim data is based on atomic H emissions with the protons and H in collisional equilibrium. Solar Probe, by measuring the pickup ions due to hydrogen, can confirm the validity of this technique (for example the flow, wave and thermal motion for protons could be greater than H if collisional coupling is not complete).

3.3 Acceleration and transport of energetic particles

When a flare occurs and coronal mass ejection follows, it is believed that most of the charged particle acceleration occurs high up in the corona (Tylka *et al.*, 2005). The reconnection process is not sufficient to accelerate charged particles to their observed energies. This problem can be solved if there is a sufficient seed population of suprathermal particles residing in the large coronal loops (Simnett, 2006). Furthermore, at $r \sim 3 R_S$ the Alfvén speed is expected to maximize with $V_A \sim 1000$ km/s near the equator and shocks from the CME will tend to form at heights $r > 3 R_S$. The shocks are expected to accelerate this seed population to energetic particle energies (Kahler, 2001; Mason *et al.*, 1999; Gopalswamy *et al.*, 2004). Solar Probe will probably not observe a CME near perihelion, however it will measure the seed populations near perihelion as it crosses the equatorial plane of the Sun. Furthermore, the NGS instrument will be able to measure neutron and γ -rays coming from nanoflares ($\sim 10^{24}$ ergs) which cannot be observed at the Earth. Neutrons decay well before they reach the Earth. The approximate location of the flare site can be determined since the γ -rays

arrive instantaneously, while the slower moving neutrons arrive later and the time-of-flight will give the flare's approximate location. In a statistical sense, these observations may then be compared with *in situ* observations of nanoflares or ion jets, thereby confirming, or not, the nanoflare model of Parker for heating the corona.

3.4 Dusty plasma phenomena and inner source for energetic particles

The dust environment surrounding the Sun is largely unknown (see Mann et al., 2004). But, it is known to produce the F corona observed by coronagraphs and is the primary cause for the zodiacal light. The dust is believed to come from comets and asteroids that venture to the inner heliosphere. Dust particle trajectories are believed to decay inward via the Poynting-Robertson deceleration and dust particle collisions may be important. As they diffuse inward, they essentially vaporize at a distance, $r \sim 2 R_S$, inside that probed by Solar Probe (see Mann et al., 2004). The dust particles are expected to be near the equatorial plane and move around the Sun in the prograde direction. Dust particles will acquire a charge and the very small particles \sim micron or less, will be affected by electromagnetic forces and execute complex trajectories around the Sun (Mann et al., 2000). The composition of the dust particles are essentially unknown, and may be the "inner source" of pickup ions that are accelerated and observed by the SWICS experiment on Ulysses (Geiss et al., 1996). Solar Probe will measure the number of dust particles as it moves in radius and latitude around the Sun and give us our first close view of the dust environment.

4. Human exploration and space weather applications

Solar Probe will provide ground truth observations of remote sensing observations of the Sun's corona and near solar wind. Manned missions to the moon and Mars will require a network of remote sensing and *in situ* measurements of the inner heliosphere and near Earth solar wind, in order to develop a reliable space weather monitoring and prediction capability to ensure astronaut safety. A major solar flare during an EVA (extra vehicular activity) could be fatal to astronauts. Without a reliable space weather capability, astronaut movement outside their capsules will be greatly limited. As outlined above, the corona and source region inside the Alfvén critical point could have a highly filamentary structure, high wave activity, numerous ion beams or jets from nanoflares (produced locally and non-locally) and electron strahl, just to name a few. Without Solar Probe *in situ* and remote sensing observations within the corona and inner heliosphere, the ability to develop reliable remote sensing observations of the Sun's corona for space weather applications, may never be achievable.

Acknowledgements. The technical material in this paper was taken from the Solar Probe STDT (NASA/TM-2005-212786; see <http://solarprobe.gsfc.nasa.gov/>). Critical contributions to that effort were made by all members of the STDT and an engineering support team from the Johns Hopkins University

Applied Physics Laboratory, as well as a number of outside scientists and engineers (see acknowledgements in the STDT report).

References

- J. W. Belcher, "Alfvénic wave pressures and the solar wind", *Astrophys. J.*, vol. 168, pp. 509-524, 1971.
- S. R. Cranmer, G. B. Field and J. L. Kohl, "Spectroscopic constraints on models of ion cyclotron resonance heating in the polar solar corona and high-speed solar wind", *Astrophys. J.*, vol. 518, pp. 937-947, 1999.
- S. R. Cranmer and van Ballegoijen, "On the generation, propagation, and reflection of Alfvén waves from the solar photosphere to the distant heliosphere", *Astrophys. J. Supp.*, vol. 156, pp. 265-293, 2005.
- J. Geiss, G. Gloeckler and R. V. Steiger, "Origin of the solar wind from composition data", *Space Sci. Rev.*, vol. 72, pp. 49-60, 1995.
- J. Geiss, G. Gloeckler and R. V. Steiger, "Origin of C⁺ ions in the heliosphere", *Space Sci. Rev.*, vol. 78, p. 43, 1996.
- N. Gopalswamy et al., "Intensity variation of large solar energetic particle events associated with coronal mass ejections", *J. Geophys. Res.*, vol. 109, A12105, pp. 1-18, 2004.
- J. V. Hollweg, "Hydromagnetic waves in interplanetary space", *Astron. Soc. Pacific*, vol. 86, p. 561, 1974.
- J. V. Hollweg, "Alfvén waves in the solar atmosphere", *Solar Phys.*, vol. 56, p. 305, 1978.
- J. V. Hollweg and P. A. Isenberg, "Generation of the fast wind: A review with emphasis on the resonant cyclotron interaction", *J. Geophys. Res.*, vol. 107, pp. 1-37, doi:10.1029/2001JA000270, 2002.
- S. W. Kahler, "The correlation between solar energetic particle peak intensities and the speeds of coronal mass ejections: Effects of ambient particle densities and energy spectra", *J. Geophys. Res.*, vol. 106, pp. 20947-20955, 2001.
- J. L. Kohl, et al., "UVCS/SOHO empirical determinations of anisotropic velocity distributions in the solar corona", *Astrophys. J.*, vol. 501, pp. L127-L131, 1998.
- I. Mann, A. Krivov and H. Kimura, "Dust cloud near the Sun", *Icarus*, vol. 146, pp. 568-582, 2000.
- I. Mann et al., "Dust near the Sun", *Space Sci. Rev.*, vol. 110, pp. 269-305, 2004.
- G. M. Mason et al., "³He enhancements in large solar energetic particle events", *Astrophys. J.*, vol. 525, pp. L133-L136, 1999.
- W. H. Matthaeus, G. P. Zank, S. Oughton, D. J. Mullen and P. Dmitruk, "Coronal heating by magnetohydrodynamic turbulence driven by reflected low-frequency waves", *Astrophys. J.*, vol. 523, pp. L93-L96, 1999.
- D. J. McComas et al., "The three-dimensional solar wind around solar maximum", *Geophys. Res. Lett.*, vol. 30, 1517, 24 pp. 1-4, doi:10.1029/2003GL017136, 2003.
- D. J. McComas et al., "Understanding coronal heating and solar wind acceleration: The case for near-Sun measurements", *Rev. of Geophys.*, in press, 2006.
- E. N. Parker, "Dynamics of the interplanetary gas and magnetic fields", *Astrophys. J.*, vol. 128, pp. 644-675, 1958.
- E. N. Parker, "Nanoflares and the solar x-ray corona", *Astrophys. J.*, vol. 330, p. 474, 1988.
- E. N. Parker, "Heating solar coronal holes", *Astrophys. J.*, vol. 372, p. 719, 1991.
- D. A. Roberts, "Interplanetary observational constraints on Alfvén wave acceleration of the solar wind", *J. Geophys. Res.*, vol. 94, pp. 6899-6905, 1989.
- N. A. Schwadron, L. A. Fisk and T. H. Zurbuchen, "Elemental fractionation in the slow solar wind", *Astrophys. J.*, vol. 521, pp. 859-867, 1999.
- G. M. Simnett, "The search for a causal link between CMEs and large flares", this issue, 2006.
- A. J. Tylka et al., "Shock geometry, seed populations, and the origin of variable elemental composition at high energies in large gradual solar particle events", *Astrophys. J.*, vol. 625, pp. 474-495, 2005.
- Y. -M. Wang, N. R. Sheeley Jr., J. L. Phillips and B. E. Goldstein, "Solar wind stream interactions and the wind speed-expansion factor relationship", *Astrophys. J.*, vol. 488, pp. L51-L54, 1997.
- T. H. Zurbuchen, L. A. Fisk, G. Gloeckler and R. von Steiger, "The solar wind composition throughout the solar cycle: A continuum of dynamic

states”, *Geophys. Res. Lett.*, vol. 29, 66-1-4,
doi:10.1029/2001GL013946, 2002.